Tests of innovative photon detectors and integrated electronics for the large-area CLAS12 RICH

M. Contalbrigo
(on behalf of the CLAS12 RICH Group)

INFN Sezione di Ferrara and University of Ferrara, Italy

Abstract

A large area ring-imaging Cherenkov detector has been designed to provide clean hadron identification capability in the momentum range from 3 GeV/c to 8 GeV/c for the CLAS12 experiments at the upgraded 12 GeV continuous electron beam accelerator facility of Jefferson Lab, to study the 3D nucleon structure in the yet poorly explored valence region by deep-inelastic scattering, and to perform precision measurements in hadron spectroscopy.

The adopted solution foresees a novel hybrid optics design based on an aerogel radiator, composite mirrors and densely-packed and highly-segmented photon detector. Cherenkov light will either be imaged directly (forward tracks) or after two mirror reflections (large angle tracks).

Extensive tests have been performed on Hamamatsu H8500 and novel flat multi-anode photomultipliers under development and on customized matrices of Hamamatsu SiPM matrices. A large scale prototype based on 28 H8500 MA-PMTs has been realized and tested with few GeV/c hadron beams at the T9 test-beam facility of CERN. In addition a small prototype was used to study the response of SiPM matrices within a temperature interval ranging from 25 down to -25 Celsius degrees. The preliminary results of the individual photon detector tests and of the prototype performances at the test-beams are here reported

Keywords: Cherenkov radiation, Multi-anode photomultipliers, Silicon photomultiplier, proximity-focusing RICH, Aerogel

1. Introduction

The CLAS12 detector at Jefferson Lab (JLab) (VA, USA), after the ongoing accelerator upgrade, will receive polarised electron beams of maximum energy 11 GeV and luminosity up to 10^{35} cm^{-2}s^{-1}, providing a world-leading facility for the study of electron-nucleon scattering with nearly full angular coverage [1]. The physics program is extremely broad [2] but, in particular, will focus upon 3D imaging of the nucleon through the mapping of generalized and transverse momentum dependent parton distributions at unprecedented high Bjorken x [3]. In particular three approved experiments demand an efficient hadron identification across the momentum range from 3 to 8 GeV/c, not covered by the existing time-of-flight system (TOF), and scattering angles up to 25 degrees. A pion rejection power of about 1:500 is required to limit the pion contamination in the kaon sample to a few percent level. A ring-imaging Cherenkov detector (RICH), instrumenting at least two symmetric CLAS12 radial sectors out of the total six, is under construction to achieve the needed hadron identification and accomplish the physics program. The radial sectors have a projective geometry, a depth of 1.2 m and about 5 m^2 entrance window area. Simulation studies favor a hybrid imaging RICH design incorporating aerogel radiators, visible light photon detectors, and a focusing mirror system [4].

The best radiator for RICH hadron identification in the few GeV momentum range is silica aerogel, an amorphous solid network of SiO_2 nanocrystals with a very low macroscopic density and a refractive index in between gases and liquids. It has been successfully used as radiator material for RICH detectors in several particle physics experiments [5] and is planned for future use [6].

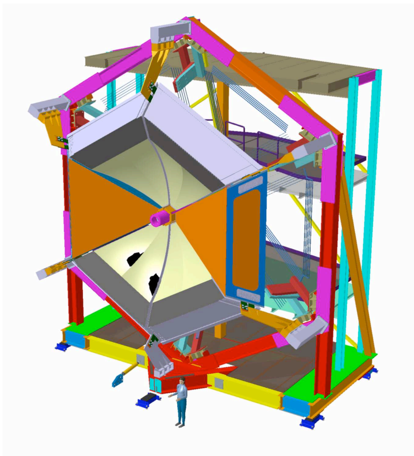

Figure 1: The two-sector baseline RICH detector (orange) positioned in place of the low threshold Cherenkov counters in the forward section of the CLAS12 spectrometer.

A focusing mirror system will be used to reduce the detection area instrumented by photon detectors to about 1 m^2 per

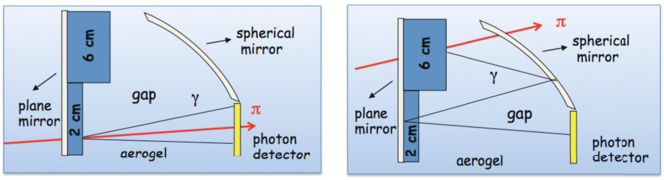

Figure 2: The CLAS12 hybrid optics design (see text for details).

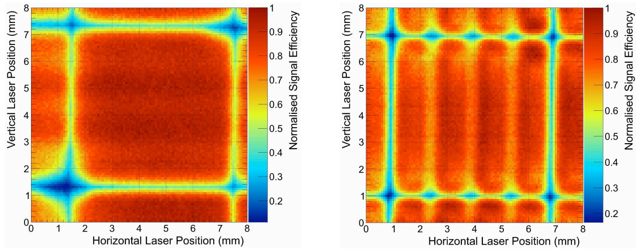

Figure 3: Normalized response map of a H8500 (left) and a H12700 (right) MA-PMT, obtained by scanning a 8×8 mm^2 area with a pico-second pulsed laser spot of 90 μm diameter and 635 nm wavelength with step size of 80 μm.

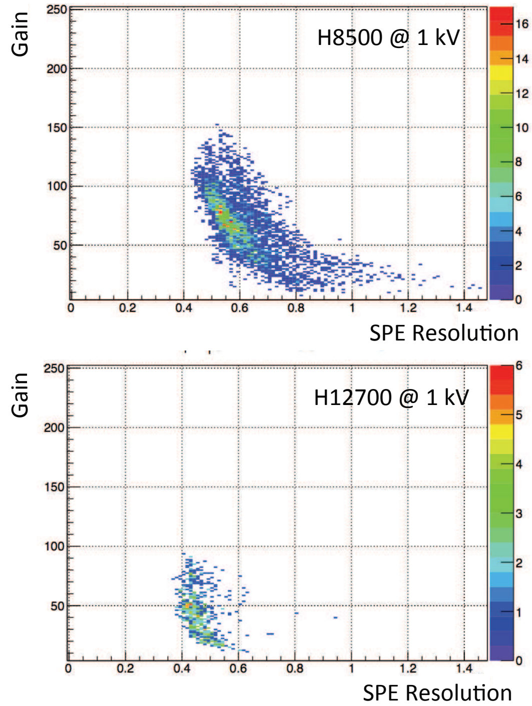

Figure 4: Gain (in terms of ADC channels) versus single photoelectron signal resolution (defined as rms over distance from pedestal ratio of the single photon electron signal) for the readout channels of the tested H8500 (top) and H12700 (bottom) devices operated at 1000 V and illuminated by a 405 nm laser wavelength.

sector, minimizing costs and influence on the detectors (TOF and Calorimeters) positioned behind the RICH, see Fig. 2. For forward scattered particles ($\theta < 13^o$) with momenta p = 3 - 8 GeV/c, a proximity imaging method with thin (2 cm) aerogel and direct Cherenkov light detection will be used. For larger incident particle angles of $13^o < \theta < 35^o$ and intermediate momenta of p = 3 - 6 GeV/c, the Cherenkov light will undergo two reflections and further passes through the thin radiator material before detection. The longer path of light and the focusing mirror allow the use of thick (6 cm) aerogel to compensate yield losses in the thin radiator.

As confirmed by simulation studies [4], the photon detector must provide a spatial resolution of less than 1 cm to not degrade the Cherenkov angle resolution in the CLAS12 RICH geometry. The fringe field of the CLAS12 torus magnet along the photon detector plane is evaluated of the order of few gauss, allowing the use of standard multianode photomultipliers (MA-PMTs).

2. The H8500 MA-PMT and the large-size RICH prototype

The Hamamatsu H8500 multianode photomultiplier tubes have been selected as a candidate being an effective compromise between detector performance and cost. It comprises an 8×8 array of pixels, each with dimensions 5.8 mm $\times$ 5.8 mm, into an active area of 49.0 mm $\times$ 49.0 mm with a very high packing fraction of 89%. The device offers a spectral response matching the spectrum of light transmitted by the aerogel, with a quantum efficiency peaking at 400 nm, and a fast response (less than 1 ns rise time) useful to suppress background.

Although the H8500 MA-PMT is not advertised as the optimal device for single photon detection purposes, several units have been characterized in laboratory tests achieving performances adequate to the CLAS12 RICH requirements [7].

Testbeam studies of a large-size prototype RICH detector were performed at the T9 beam line in the CERN-PS East Area, with a mixed hadron beam of 6-8 GeV/c momentum. Two setups were mounted inside a $\sim$ 1.5 m wide light-tight box to study direct and reflected light imaging modes individually. The Cherenkov light was detected by 28 MA-PMTs mounted along a circular array and could be radially moved to intercept the Cherenkov ring produced with different opening angles depending on the chosen refractive index. The test-beam set-up was completed by a tracking system consisting into two gaseous electron multipliers chambers with 10x10 cm^2 area and a threshold Cherenkov CO_2 gas counter to tag pions. The prototype readout electronics was based on the MAROC3 [8] chip and derived from medical imaging applications. Each 5×5 cm^2 Front-End MAROC card served a 64 channel multi-anode PMT. The controller board could host up to 64 Front-End cards allowing to concentrate thousands of readout channels in a very compact layout.

The direct light case reproduces the 1 m gap of the CLAS12 geometry. In the early stages of data analysis, an average yield of 12 photo-electrons and a π/K separation close to the goal value of 4σ in units of Cherenkov angle resolution have been obtained with a 2 cm n=1.05 aerogel up to the maximum beam momentum of 8 GeV/c.

In the reflected light RICH configuration, no significant degradation of the net Cherenkov angle resolution was observed on top of the expected 60% light yield loss effect due to the

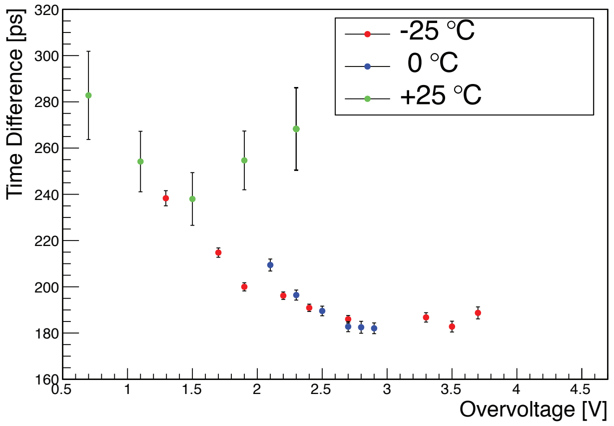

Figure 5: Time difference rms between SiPM hits collected within ± 3 ns from the trigger time as a function of the overvoltage, at three different temperatures.

aerogel transmission. These preliminary results validate the CLAS12 RICH concept [9].

3. The novel H12700 MA-PMT

The CLAS12 RICH unconventional geometry with multiple light passes through the radiator demands a high photon detection efficiency. Recently the novel Hamamatsu H12700 multi-anode PMT has become available, with the same layout as the H8500 but optimized dynode structure for single photon detection, see Fig. 3. Several H12700 units have been tested illuminating each pixel center with a pico-second pulsed laser spot of ∼ 1 mm diameter and 465,5 nm wavelength, yielding promising results in terms of single photon resolution despite the slightly reduced gain, see Fig. 4. Although, in some cases, the border pixels of the H12700 device show a significant increase of the dark current with respect the typical H8500 values, the corresponding dark counts are limited to values of no concern for the CLAS12 RICH application. Most important for Cherenkov applications, the new dynode structure is expected to provide an enhanced catode sensitivity and a better collection efficiency: the tested H12700 MA-PMT yield a single photon-detection efficiency in average 25% higher than the standard H8500.

4. The Silicon-Photomultiplier Option

The fast developing silicon photomultipliers represent a possible cost-effective alternative for upgrades of the detector. A small prototype was used to study the performance of 3 × 3 mm^2 silicon multi-pixel photon counter (MPPC) matrices with a 3 cm n=1.05 aerogel and 36 cm gap. A commercial 8 × 8 MPPC matrix was compared to two customized 8 × 4 MPPC matrices with an embedded pre-amplification stage. All the matrices were temperature controlled by means of water cooled Peltier cells. The response to Cherenkov light was studied within a temperature interval ranging from 25 down to -25 degrees Celsius. The SiPM matrices were operated inside a black box in a dry nitrogen atmosphere to avoid water condensation at low temperature. Each SiPM was connected to the external Front-End electronics by a 1.5 m coaxial cable. The amplification and discrimination stage of the SiPM signals were derived from an electronic R&D of the SuperB muon detector. The discriminated signal were fed to a 128 channel V1190A CAEN TDC with a 100 ps time resultion. The MPPC signal hits were selected by a relatively broad trigger time coincidence of ±3 ns, driven by the external trigger jitter, which limited the dark count background rejection. Anyway, at low temperature, a stable and uniform response could be achieved in a large interval of bias voltage and discriminating threshold values: a 30-40% higher than H8500 single photon detection efficiency was recorded while approaching a manageable 10^{-4} dark count background occupancy [9].

The width of the time difference distribution between SiPM hits in the same event provides an estimate of the SiPM signal time resolution as removes the trigger jitter while getting negligible contribution from the different photon paths. Despite the system was not design for excellent time performances, the preliminary analysis indicates a time difference rms as low as 180 ps, see Fig. 5, corresponding to a time resolution σ_t of the order of 130 ps, at low temperature and high overvoltage. By rejecting the hits outside a window of $3\sigma_t$ centered on the average SiPM hit time, a further reduction of the the combinatorial background in each event was obtained, reflecting in a overall 10% improvement in the Cherenkov angle resolution.

The above results validate the use of SiPM as single photon detectors. However, SiPMs are known for their limited tolerance to the radiation damage and dedicated irradiation tests had to be performed to validate their use for the CLAS12 RICH application. Geant4 simulation of the CLAS12 environment indicate that the neutron fluence at the RICH detector position is moderate, at the level of few 10^9 n_{eq}/cm^2 per year at the maximum possible luminosity of 10^{35} $cm^{-2}s^{-1}$, where n_{eq} is the equivalent flux of 1 MeV neutrons derived from the damage curve in Fig. 6. Dedicated neutron irradiation tests were made at the Frascati Neutron Generator (FNG) of ENEA, which exploits the $T(d, n)\alpha$ reaction to produce an isotropic flux of 10^{11} neutrons per second of 14 MeV energy.

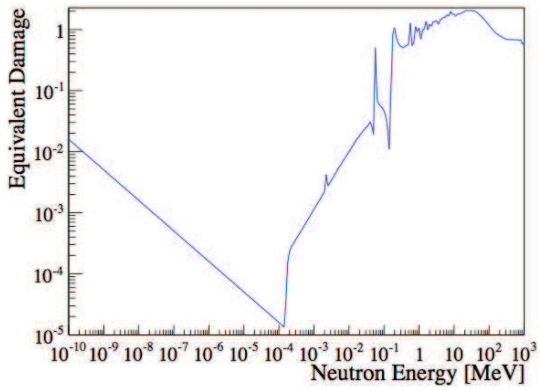

Figure 6: Effective damage to SiPM relative to 1 MeV neutron [10].

Several SiPM types from different producers were irradiated.

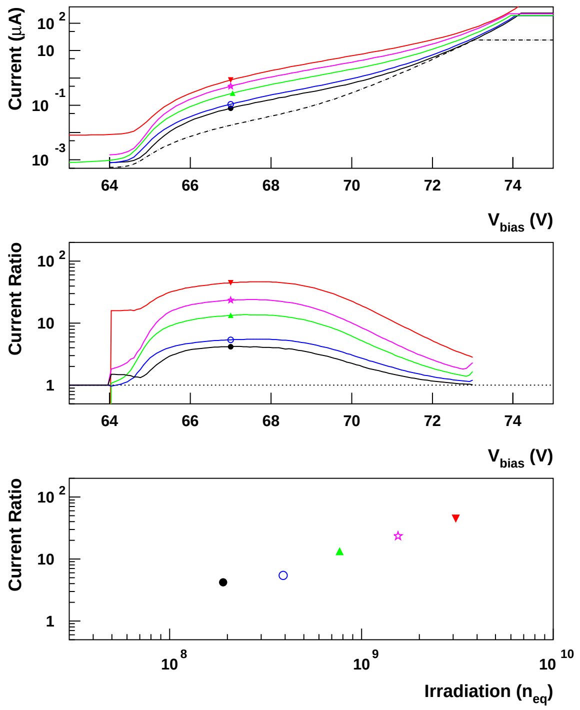

Figure 7: Response of a $3 \times 3\text{mm}^2$ Hamamatsu S12572-015-P MPPC with 15 μm micro-cells at different integrated neutron equivalent dose (marked by the different symbols). Top: current vs voltage characteristic curves compared to the one before irradiation (dashed line). Center: current ratio over the un-irradiated case. Bottom: current ratio at a 67 V bias voltage.

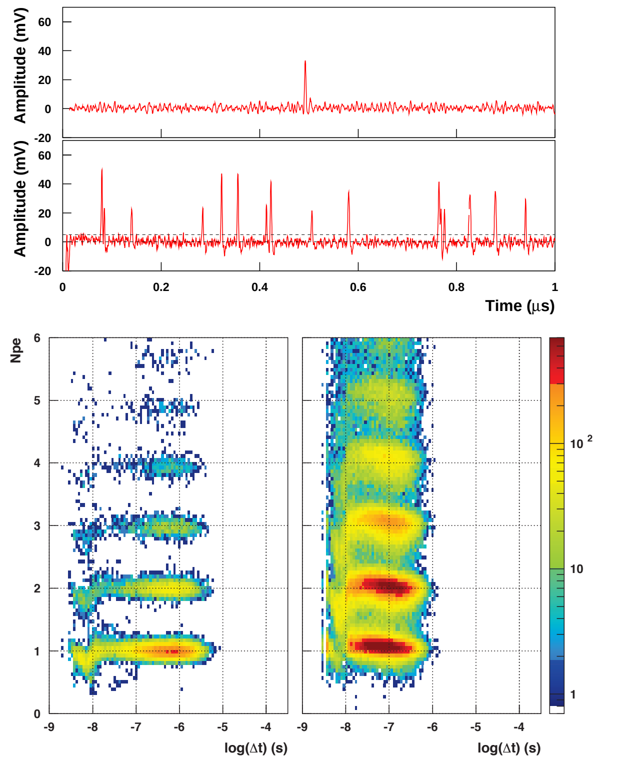

Figure 8: Top: the sampled dark-count signal of a 3×3 mm^2 Advansid ASD-RGB3S-P-50 SiPM with 50 μm micro-cells before irradiation at 22^o (upper panel) and after $3 \cdot 10^9$ n_{eq}/cm^2 dose at 0^o (lower panel) temperature. Bottom: the normalized amplitude as a function of the time distance before (left) and after (right) irradiation for the identified dark-count events.

For each type, 5 equivalent SiPM were available to be exposed to different neutron doses. The integrated dose varies from a minimum of $3 \cdot 10^8$ n_{eq}/cm^2 up to a maximum of $3 \cdot 10^9$ n_{eq}/cm^2, the latter corresponding to few years of CLAS12 run at the luminosity planned for the experiments demanding the RICH.

The SiPM response before and after the irradiation was analyzed at different temperatures. The current versus voltage characteristic curve was measured by a Keithley 6487 picoamperometer. The SiPM dark-count signals were pre-amplified by an Advansid ASD-EP-EB-N evaluation board and sampled at 2.5 Gs/s over a 10 ms time window by a Tektronik DPO 7254 oscilloscope. The analysis of the sampled signal is made in two steps [11]. In the first step, a software filter is applied, to remove the slow tail due to the SiPM cell recharge after each break-down and the following singal undershoot, and to better isolate the single dark-count events. In the second step, the dark-counts are identified as signal peaks above a given threshold and their amplitude, width and time distance from the previous peak recorded.

As expected, a sizeable increase in the dark current is found for all the tested SiPM, see an example in Fig. 7. Nevertheless, even at the maximum dose, the single dark-counts can still be isolated from the sampled signal, when the SiPM is operated at low temperature as expected for the real experiment. This is shown by the distribution of normalized peak amplitude versus time-distance of the identified dark-count events, see Fig. 8.

In conclusion a RICH detector is under construction for the CLAS12 experiment with an innovative mirror configuration to minimize the instrumented area. A front-end electronics is under development able to readout either the described MA-PMTs or SiPM matrices. It is based on the MAROC3 chip featuring 64 fast-shaped binary outputs with better than 100 ps time jitter [8] with, in addition, a slow-shaped multiplexed analog output for test and calibration. From the performed tests, the Hamamatsu H8500 MA-PMT has proven to be suitable for Cherenkov applications despite it is not designed for single photon detection and has been initially selected as a good compromise between cost and performace. An improved photon detection efficiency is expected by using the novel H12700 multianode PMTs now commercially available. For the CLAS12 RICH detector upgrades the SiPM technology appears to be a valid alternative to contain cost and material budget given the moderate particle fluence expected in the CLAS12 environment.

References

[1] CLAS12 Technical Design Report, version 5.1 208 (2008).
[2] J. Dudek *et al.*, *Eur.Phys.J.* **A48** (2012) 187.
[3] H. Avakian *et al.*, *arXiv:1202.1910v2* **[hep-ex]** (2012)
[4] M. Contalbrigo *et al.*, *Nucl. Instrum. Meth.* **A 639** (2011) 302.
[5] R. De Leo *et al.*, *Nucl. Instrum. Meth.* **A 595** (2008) 19; A. Yu. Barnyakov *et al.*, *Nucl. Instrum. Meth.* **A 453** (2000) 326; R. Pereira *et al.*, *Nucl. Instrum. Meth.* **A 639** (2011) 37; R. Forty *et al.*, *Nucl. Instrum. Meth.* **A 8923** (2010) 294.

[6] T. Iijima *et al.*, *Nucl. Instrum. Meth.* **A 598** (2009) 138;
A. Yu. Barnyakov *et al.*, *Nucl. Instrum. Meth.* **A 732** (2013) 352.
[7] R. A. Montgomery *et al.*, *Nucl. Instrum. Meth.* **A 695** (2012) 326;
M. Hoek *et al.*, eprint arXiv:1409.3622.
[8] S. Blin *et al.*, *IEEE Nucl. Sci. Symp. Conf. Rec. 2010* (2010) 1690.
[9] M. Contalbrigo *et al.*, *Nucl. Instrum. Meth.* 10.1016/j.nima.2014.06.072.
[10] Y. Qiang, *et al.*, *Nucl. Instrum. Meth.* **A 698** (2013) 234.
[11] C. Piemonte *et al.*, *Conference Record of NSS/MIC 2012*, IEEE, 2012 , pp. 428-432.